Hindawi
International Journal of Antennas and Propagation
Volume 2022, Article ID 6011557, 9 pages
https://doi.org/10.1155/2022/6011557

Research Article

Broadband Multipolarized Reconfigurable Unit Cell for Reflectarray Antennas with One Bit Control

Hoang Dang Cuong,[1] Minh Thuy Le ,[2] Trong Toan Do,[3] and Nguyen Quoc Dinh[1]

[1]*Le Quy Don Technical University, Ha Noi 100000, Vietnam*
[2]*School Electrical and Electronic Engineering, Hanoi University of Science and Technology, Ha Noi 100000, Vietnam*
[3]*Viettel High Technology Industries Corporation, Ha Noi 100000, Vietnam*

Correspondence should be addressed to Minh Thuy Le; thuy.leminh@hust.edu.vn

Received 5 February 2022; Revised 23 March 2022; Accepted 28 March 2022; Published 14 April 2022

Academic Editor: Eng Hock Lim

A broadband and multipolarized fully reconfigurable unit cell is designed and fabricated in this paper. The unit cell uses 4 diodes to create a phase shifter with single-bit control. It exhibits an excellent bandwidth of 40% for both dual linear and circular polarizations in the *X* and Ku bands using the structure of 4 patches, a proper PIN diode placement, and a DC bias. The reflection coefficients of the cross polarizations are less than −50 dB, ensuring high isolation between the two polarizations. The experiment results show an agreement with the simulation results.

1. Introduction

The advantages of microstrip reflectarrays (RFAs) are low cost, low weight, low profile, and planar compared to the parabolic reflector. In millimeter wave, RFA uses the air feeding to avoid the high loss in the feeding network. For the beamforming purpose, RFA does not use RF modules and ADC and DAC blocks which cause the system more complicated and costly like the traditional phased array antenna. Therefore, RFAs could be a candidate for a replacement of the phase arrays in satellite communications [1–3], radars, point to point terrestrial links, 5G [4, 5], and beyond. However, the limited bandwidth (BW) of RFAs which inherited from microstrip antennas is one disadvantage [6]. Moreover, the air feeding structures cause differential spatial phase delay which degrade their bandwidth, especially for moderate and large-sized reflectarrays [6]. Recently, the BW of RFAs has been improved significantly, up to 26.7% (-1 dB BW) in [7], 33.52% (-1 dB BW) in [8], and 28.8% (-1 dB BW) in [9]. The key techniques to improve the BW of the RFAs are lowering the phase sensitivity of elements by combining various structures in an element or using different types of unit cell in an array [10, 11]; the spatial dispersion is compensated by dividing the array to independent zones for optimizing reflective phases [9, 10].

The reflectarray (RFA) has the capability of beamforming namely reconfigurable reflectarray (RRA). RRAs are designed by changing the phases of reflecting elements, which are controlled by one or two bits. As RFAs, they can be used for civilian and military applications, especially in satellite communication and radar with the requirement of steering [12]. Recently, passive RIS (reconfigurable intelligent surfaces) or intelligent reflecting surface (IRS) with a large number of reflective elements is coming up as a promising candidate for next generation antennas [13, 14]. The principle of these antennas is similar to the RRA, and their feeders are base stations instead of horn antennas. Their elements are also reconfigurable unit cells with one or two bits controlling.

The integrated solid-state devices such as PIN diodes, varactor diodes, MEMs, and crystal liquid are typically used to control the phases of elements in the RRAs [15]. Among them, the PIN diode is widely adopted because of the simple and low-cost controlling circuits. Besides, the diversity of PIN diodes is available on the market. Only varactor diodes

can produce a smooth phase unit cell, but they are rarely used due to the complicated and high-cost control boards [16, 17]. MEMs come with many advantages for RRAs such as small size, low insertion loss, and low power consumption [18, 19]. However, the high cost and unsteady-available manufacturing process hinder their popularity. The mechanical method is also adopted to change element phases for a specific purpose like high power [20].

The bandwidth of RRAs is affected by the structure of its feeding and unit cell structures. The air feeding structure of RRAs causes the spatial dispersion and oblique effect, and limits the bandwidth of RRAs. Thanks to the phase digitizing, the phase delay errors caused by the spatial dispersion influence the bandwidth performance of RRAs less than RFAs. Therefore, the bandwidth of RRAs is theoretically wider than the RFAs, even for large RRAs [21], and the bandwidth of RRAs with 1-bit controlling can be wider than the 2-bit RRAs [22]. However, the bandwidth of the RRAs is also significantly dependent on the bandwidth of the unit cells. As active devices and DC-bias structures are adopted on reconfigurable unit cells, they introduce parasitic parameters and insert losses. Therefore, the bandwidth of the unit cell is degraded considerably, and creating a wide bandwidth reconfigurable unit cell has still been a great demand for many decades.

Recent works have been focusing on RRAs with 1-bit and 2-bit controlling. A thorough literature review reveals that the number of published literature of RRAs using PIN diode is overweight other aforementioned methods [23–40]. Among them, 1-bit RRAs using PIN diode is receiving more attention [23–35] since they are capable of achieving a wider band than 2-bit RRAs due to simple DC-bias structures. Therefore, we focus on analyzing the bandwidth of this type of RRAs and propose a method to improve their bandwidth performance.

Most recent works used two approaches to make a phase shifter: delay lines and tunable resonator. In [23], the unit cell uses a PIN diode and a delay line to change its reflection phase. Its principle is simple, but the mismatch between the patch and the delay line limits the bandwidth of the unit cell. As a result, its bandwidth for the reflection phase from 170° to 200° is just 450 MHz at 60 GHz. The work in [26] also proposed a multipolarized RRA element using a delay line and two PIN diodes. It obtained a bandwidth of 10.5%, from 13.5 GHz to 15 GHz for a phase range of 180° ± 20°. Reference [25] presented a polarization-turning unit cell with a complicated structure. They adopted 4 PIN diodes and 4 layers for impedance matching, polarization turning, and DC isolating. This design is based on the approach of tunable resonator, which shifts the phase by altering the resonant frequency. This unit cell achieved a wideband of nearly 20% at 13.25 GHz thanks to the high isolation between DC-bias structure and the unit cell. Reference [31] showed a unit cell using two patches and one PIN diode. This work also adopted the approach of tunable resonator, but it only obtained a 180° ± 20° bandwidth of 12% at 5 GHz.

Recently, a "receiving-phase shift-transmitting" unit cell is proposed [35]. The phase shifter uses a "microstrip-slot-microstrip" structure and two diodes to reverse the current, which helps the unit cell achieve a bandwidth of 20.8%, from 11.6 GHz to 14.3 GHz. To date, because of narrow-band unit cells, the bandwidth of 1-bit RRAs using PIN diodes is still lower than RFAs, less than 16% compared to around 25% for 1-dB bandwidth [8, 9, 41]. In this paper, we proposed a novel broadband unit cell operating at *X* and Ku bands. To obtain a wide bandwidth, we adopt the approach of tunable resonator by placing 4 diodes in the middle unit cell, avoiding the mismatching between patches and delay lines. The DC-bias structure is also designed properly to eliminate the parasitic resonance.

This paper is organized as follows. Section 2 introduces the geometry and performance of the proposed unit cell. Section 3 presents the measured results with discussion. Section 4 concludes this work.

2. Design and Performance of Unit Cell

2.1. Unit Cell Design. The structure of the proposed unit cell is illustrated in Figure 1. The designed unit cell works at the *X* and Ku bands, with a dimension of 12 mm, less than a half of wavelengths in the intended frequency bands. The unit cell consists of two dielectric layers, including RT5880 and a FR4 substrates, which are bonded together by a prepreg layer PP1080 and three metallic layers. The top metallic layer consists of four identical square patches that are connected together by 4 PIN diodes, etched on a RT5880 substrate with a dielectric of 2.2 and a thickness of 3.175 mm, operates as the main resonant component. The gap between the two patches is g. The middle metallic layer works as a ground plane or a reflective surface. The bottom metallic layer contains four radial stubs printed on a FR4 substrate, choking the RF signals from the unit cell to the DC controlling board.

To understand more clearly, two equivalent circuits which model two patches connected by a diode for each polarization in x-axis or y-axis are presented on Figure 2. Due to the electrical independence of twin patches, we just model a couple of patches for the whole. As shown in Figure 2, the patch is modeled as an inductor L_p and a capacitor C_p while via is modeled as an inductor L_{v1} in series with a capacitor C_v paralleled to another inductor L_{v2}. C_v represents for the coupling between the via and the ground layer. Inductors L_{v1} and L_{v2} represent for via segments from the patch to ground and from ground to the radial stub. Because the radial stub is considered as a virtual ground, inductor L_{v2} is also connected to the ground. The diode in state "ON" is modeled as a serial circuit of a resistor of 4.2 Ω and an inductor of 50 pH, while the model for "OFF" state is a capacitor of 42 fF parallel to a resistor of 300 kΩ. Hence, when the state of the diodes switches between "ON" and "OFF," the structure of the resonant circuit of the unit cell changes, leading to adjusting the resonant frequency and the reflection phase of the unit cell.

A thick RT5880 substrate is chosen to achieve a linear phase in a wide bandwidth [42], while the FR4 and the PP1080 prepreg layer are as thin as they can be to eliminate the insert losses and unwanted parasitic resonance. The detailed dimensions of the unit cell are shown in Table 1. It

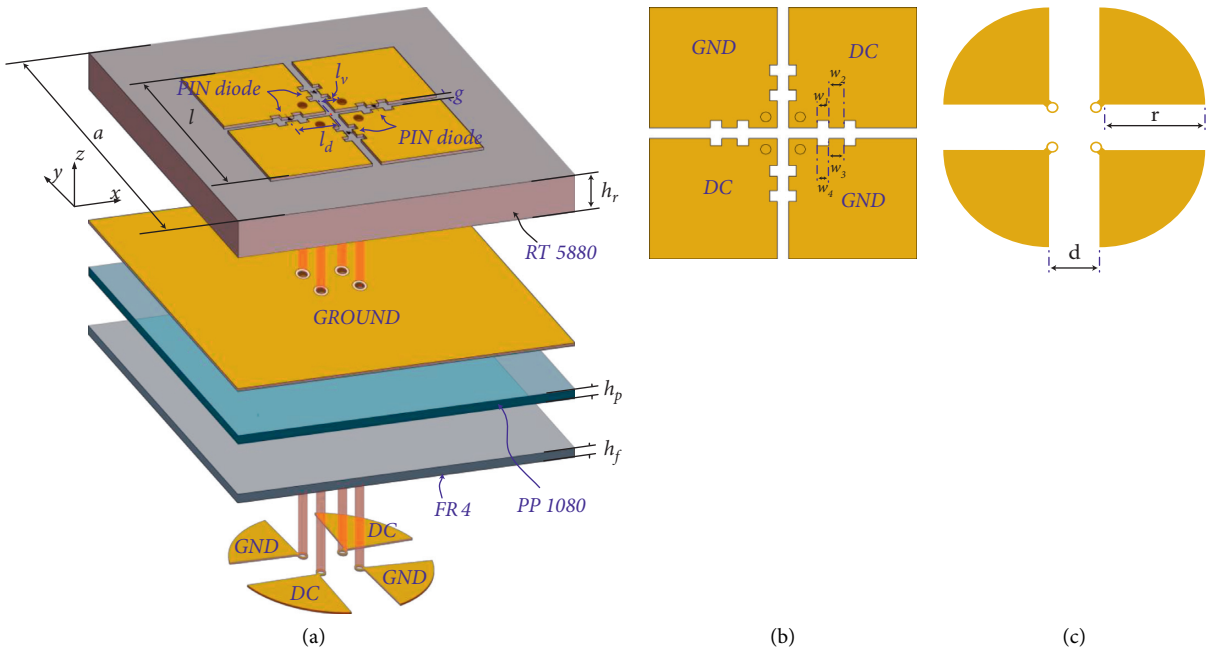

(a) (b) (c)

FIGURE 1: (a) Structure of the proposed broadband unit cell with 4 diodes on the top and 4 radial stubs on the bottom. (b) Top side of the unit cell. (c) Bottom side of the unit cell.

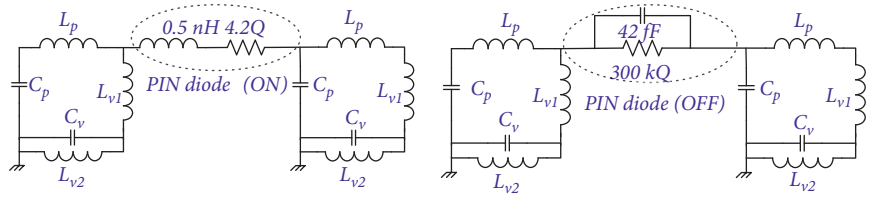

(a) (b)

FIGURE 2: The equivalent circuits of a unit cell: diode state "ON" and (a), diode state "OFF" (b).

TABLE 1: Detailed dimensions of the unit cells.

a	12	l_d	1.4	h_p	0.1	d	1.21	w_3	0.3
l	7	g	0.3	h_f	0.18	$w1$	0.2	w_4	0.2
lv	0.5	h_r	3.175	r	1.8	w_2	0.3		

unit: mm.

can be seen that placing diodes outside the patches and using delay lines for phase shifter significantly deteriorate the bandwidth of the unit cell due to the mismatch between the patches and the delay lines [26, 27, 30]. Therefore, we embedded four PIN diodes (MADP-000907-14020) in the middle of the unit cell with a distance l_v from the center. All diodes are controlled by one bit through four vias that connect 5 V or -5 V from the radial stubs to the patches. Placing four diodes symmetrically allows unit cell to operate in two orthogonal polarizations. All diodes are controlled by one bit through four vias that connect the radial stubs to the patches. To keep the symmetry of the unit cell, two vias are connected to the radial stubs and two are grounded instead of connecting all four vias to the ground layer for simplification.

The via position lv is also carefully examined to maximize the isolation between the DC-bias circuits and the RF signals. Thanks to the parametric study, authors recognize that the bandwidth of the unit cell is sensitive to the diode positions l_d. As shown in Figure 3, the bandwidth of unit cell for a phase range of $180^o \pm 20^o$ decreases significantly from 40% to 11% and 8.4% in accordance with diode positions of 1.6 mm and 1.8 mm, respectively. Hence, fixing the positions of the diodes is crucial to obtain the best performance of the unit cell. To date, wire bonding and SMT are two popular technologies that could connect such a tiny SMD diode to the top metallic layer.

As wire bonding is rare and high cost, SMT is still the best method for mounting the PIN diodes on a surface in our situation. However, the SMT process always requires the

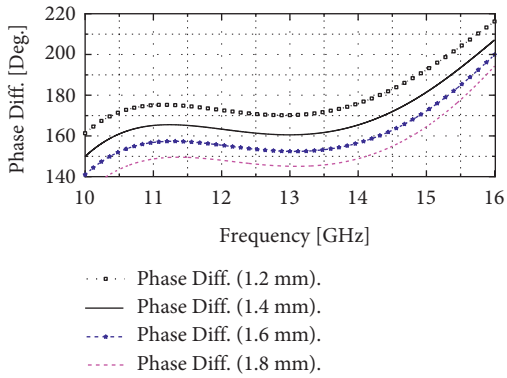

FIGURE 3: Reflection phase differences vs diode positions.

soldering masks for fixing the soldered devices, which causes the parasitic parameters. To avoid these unwanted resonances and exactly mount the diodes on the top metallic surface, authors design two slots as shown in Figure 1(b).

2.2. Dual Linear and Circular Polarization Performances. For the structure of the proposed unit cell, three parameters g, l_d, *and* l_v significantly influence the bandwidth performance of the unit cell. The unit cell is simulated by CST Studio in the periodic environment with a Floquet port. In such a boundary, it is easy to achieve the reflective coefficients and phases which are crucial parameters for an element in the RRAs. However, the farfield of a single element can be misleading because they are calculated in the volume of the virtual side walls and in a finite array. The reflection coefficients and phases of the unit cell are obtained and plotted in Figure 4. Since the designed unit cell is symmetric, the performances for x-polarized and y-polarized incidences have a minor discrepancy. Therefore, authors present the simulation results for y polarization and left-hand circular polarization (LHCP) as representations for dual linear polarizations and circular polarizations, respectively. Figures 4(a) and 4(c) are the performances for y polarization, while Figures 4(b) and 4(d) represent the LHCP. As observed in Figure 4, the unit cell has excellent performances for multi polarizations. The reflection coefficients of the unit cell are nearly zero at the state "OFF" and less than −1.5 dB at the state "ON" for both dual linear and circular polarizations. From these simulated results, it can be estimated that the radiation efficiencies of the unit cell are approximately 100% for "OFF" state and around 70% for "ON" state. It is noted that the deviation of the reflection coefficient at the state "1" is only 0.5 dB, less than 1 dB, which could make the unit cell a promising candidate for broadband RRAs. The bandwidth for phase shifts of $180^o \pm 20^o$ is from 10.4 GHz to 15.7 GHz (40.6%) for both dual linear polarization and circular polarization. The reflection coefficients for cross polarization are less than −50 dB for both linear and circular polarizations. Although the periodic environment in CST Studio does not allow to calculate the farfield exactly, but an extremely low cross-polarization level illustrates that the unit cell has a good axial ratio.

2.3. Performance of the Unit Cell in Oblique Incident Waves. Since the oblique incidence considerably affects the performances of the unit cell. The performance of the unit cell at various angles of the incident waves is analyzed. The simulated results for oblique incidence of 20^o and 30^o are plotted in Figure 5. As shown in Figure 5, for y polarization, the reflection coefficients and phases at 20^o and 30^o show a minor deviation. Their bandwidth is still more than 35%, and the cross-polarized coefficients are less than - 40 dB. For LHCP, the copolarized reflection coefficients ("ON" state) drop to – 2.2 dB and – 3.7 dB at frequencies around 12.5 GHz at 20^o and 30^o of incident wave, respectively. However, the cross-polarized reflection coefficients are still less than -10 dB from 10 GHz to 15 GHz. As a result, the bandwidths for LHCP at 20^o and 30^o are 28% (from 10 GHz to 13.3 GHz) and 45% (from 10.04 GHz to 16 GHz), respectively.

3. Fabrication and Measurements

To date, measuring the character of a unit cell by metallic waveguides is a unique method to verify the simulated performance. However, for a specific waveguide, the electromagnetic waves are reflected at the broadside waveguide walls with various angles depending on the frequency [40]. Therefore, to measure the character of the unit cell at different oblique angles, many waveguides with various dimensions need to be fabricated, which increases the cost of measuring. Typically, only a waveguide is adopted to validate the simulated results with acceptable tolerance [41]. In this paper, because the cross-polarization coefficient is minimal, just copolarization is measured.

To verify the performance of the proposed structure, the unit cell is fabricated and measured. The dimensions of the unit cell are 12 mm × 12 mm, and the operating frequency of the unit cell is in the bandwidth of the WR75 waveguide. Therefore, authors fabricate a double cell with a dimension of 24 mm × 12 mm for the measurement. However, the standard rectangular waveguide (WR-75) has a dimension of 19.05 mm × 9.525 mm that is not enough to contain the double cell.

A set of waveguide tapers that convert from WR75 dimensions to a dimension of 24 mm × 12 mm are designed and fabricated, as shown in Figure 6.

Thanks to the TRL calibration method [31], the 24 mm × 12 mm plane is calibrated as a reference plane for accuracy measurement results. The unit cell is fabricated at the lab as in Figure 7. To fabricate such a 3-layer unit cell, the authors used a press machine and prepreg PCL-FRP-370HR 1080 from Isola to bond the RT 5880 substrate and the FR4 layer. However, due to the lack of a laser drilling machine and chemicals for PTFE plating, the chemical for FR4 via-plating process is adopted. Hence, the quality of vias is not perfect. Furthermore, since the unit cell is grinded manually, the unit cell does not fit snugly to the waveguide as Figures 7(e) and 7(f). Because PCB fabricating process is complicated, just some of stage's products is shown such as masked middle layer for etching (Figure 7(a)), the sheet after lamination (Figure 7(b)), and the complete product (Figures 7(c) and 7(d)). Figures 7(e) and 7(f) present the unit

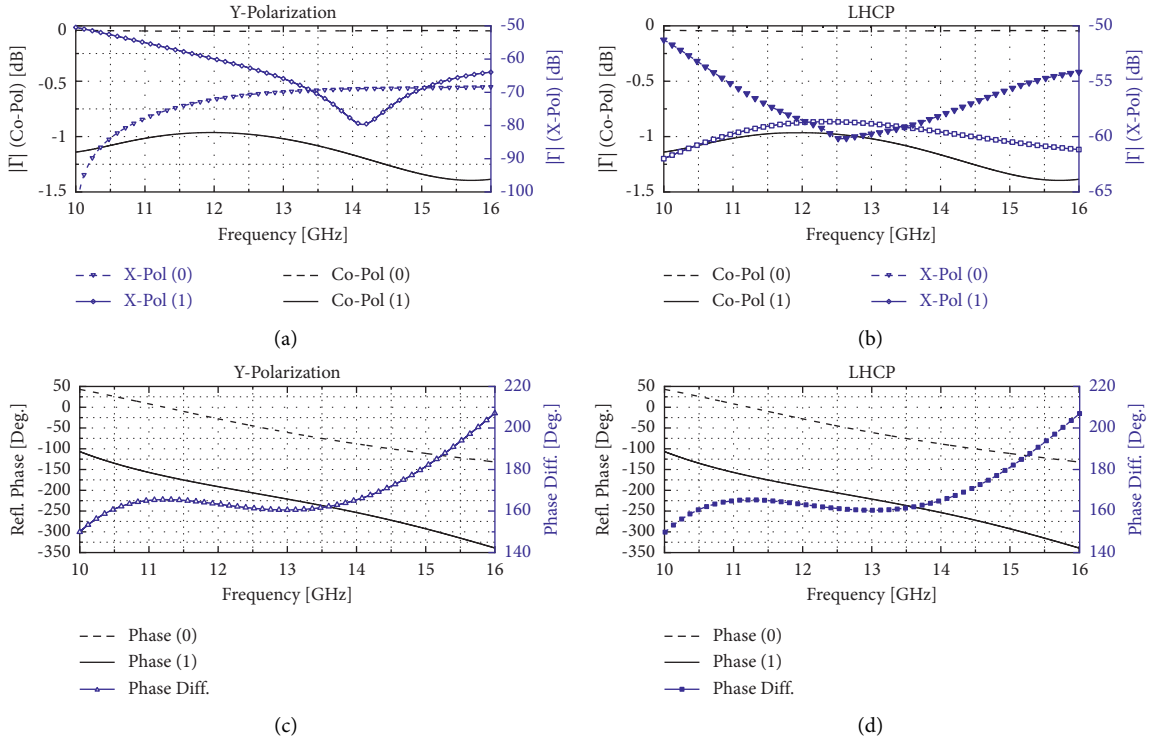

Figure 4: The simulated results: the reflection coefficient (co and cross polarization) of the unit cell for y polarizations (a), left hand circularly polarization (LHCP) (b), the reflection phase of the unit cell for y-polarizations (c), and LHCP (d). (0): "ON," (1): "OFF."

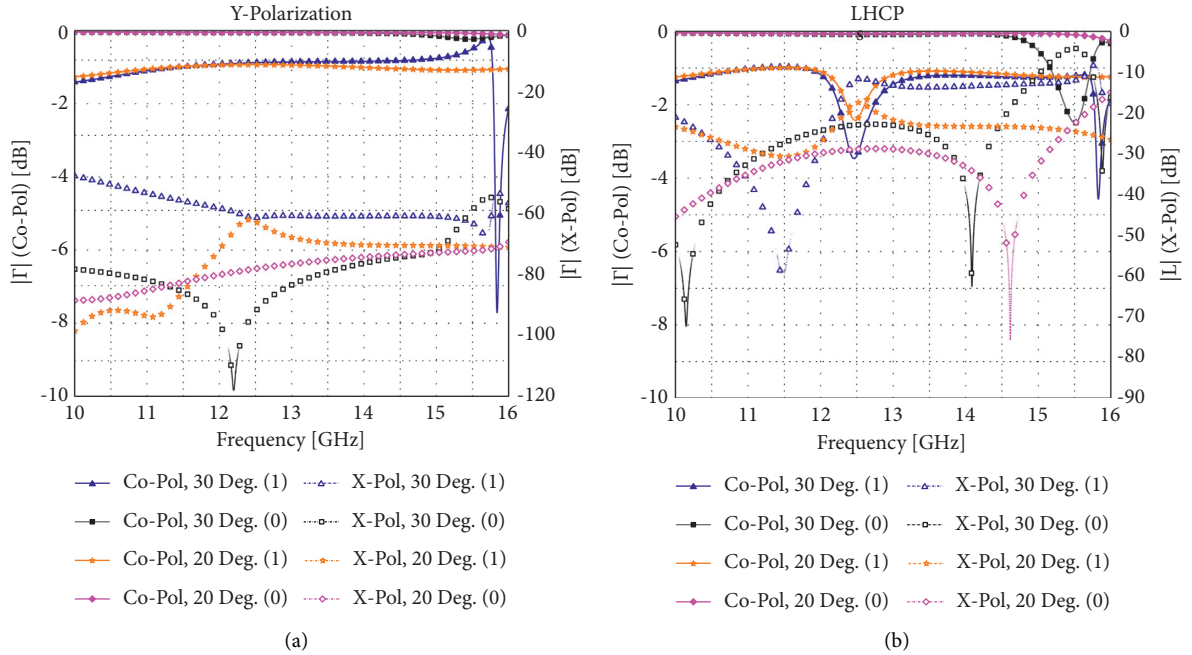

Figure 5: Continued.

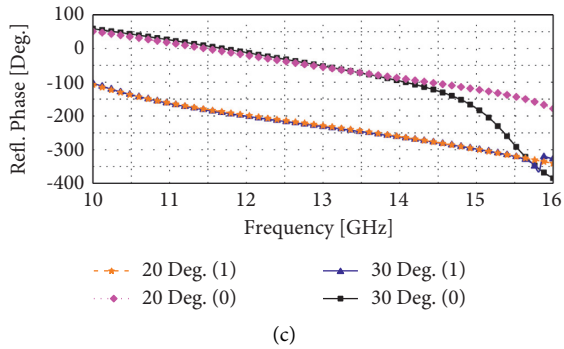

(c)

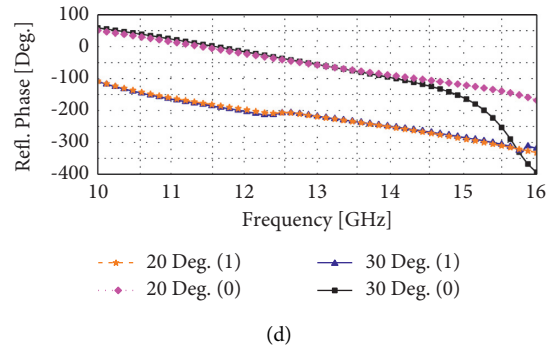

(d)

Figure 5: The simulated results in oblique incident waves: The reflection coefficient (co and cross polarization) of the unit cell at 20° and 30° for y polarizations (a) and LHCP (b). The reflection phase of the unit cell at 20° and 30° for y polarizations (c) and LHCP (d).

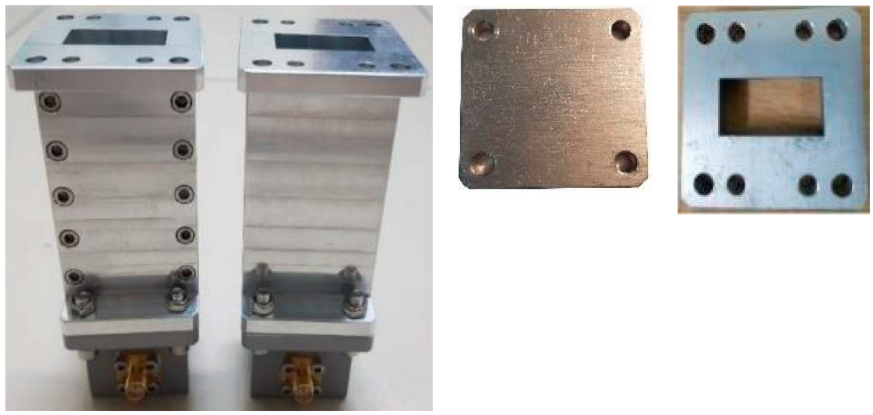

(a) (b) (c)

Figure 6: The set of WR75 taper calibration: (a) Two sets of adapter and taper. (b) Short sheet. (c) ¼ wavelength delay sheet.

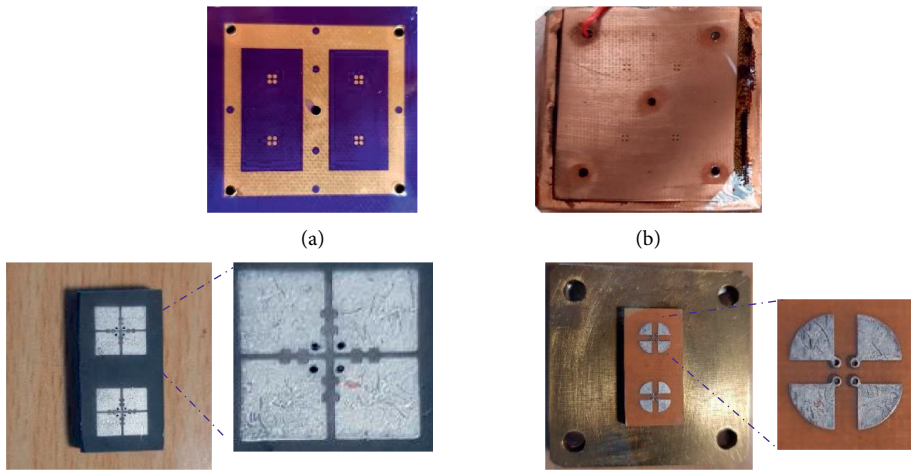

(a) (b)

(c) (d)

Figure 7: Continued.

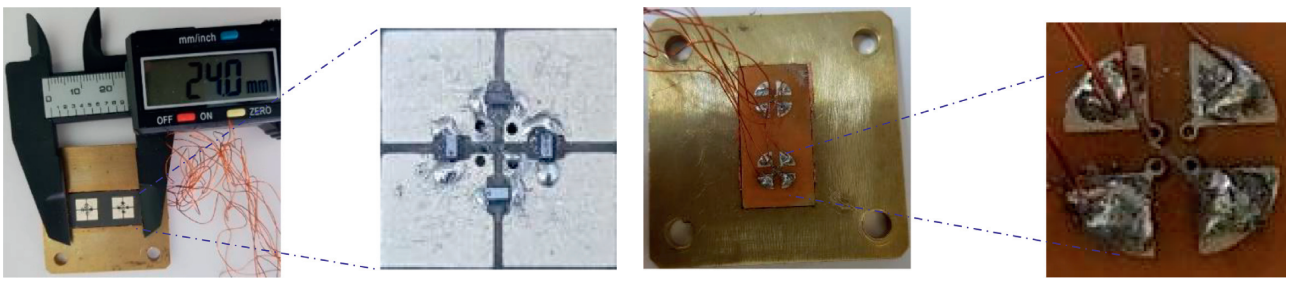

FIGURE 7: The unit cell fabrication: (a) Mask of the middle layer before etching; (b) the sheet after laminating and via plating; (c) top side and bottom side; (d) after silver plating, cutting, and grinding; (e) top side after soldering diodes; (f) bottom side with DC wires for controlling.

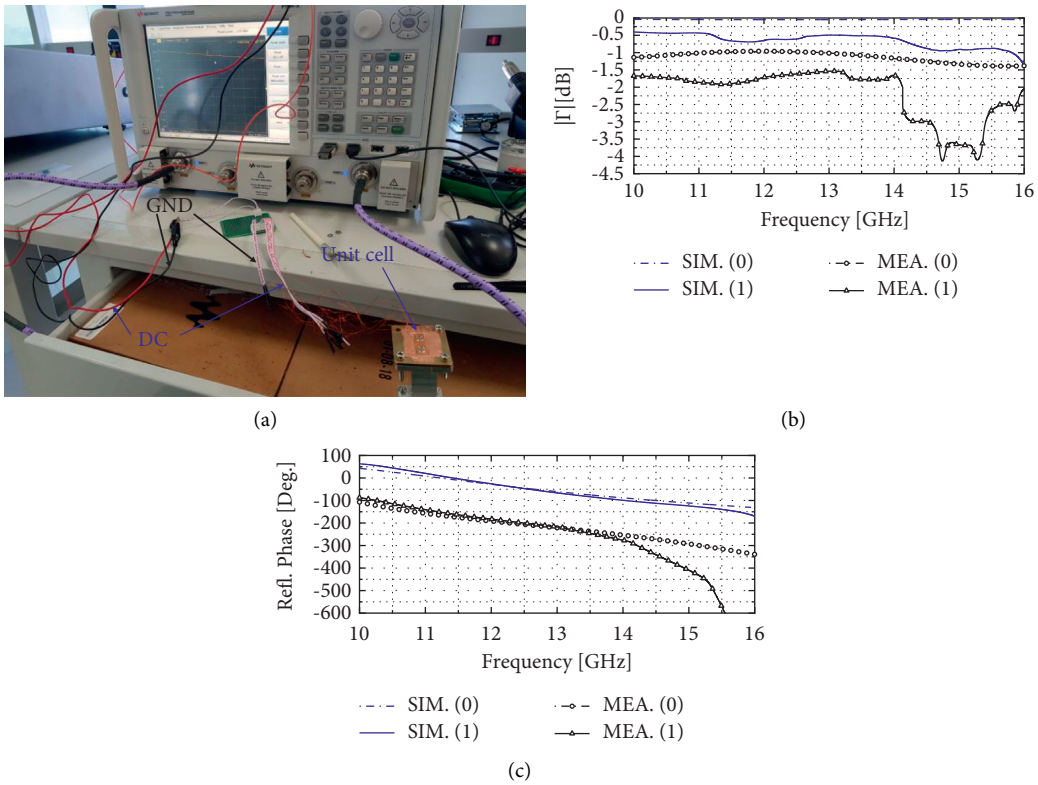

FIGURE 8: (a) Measurement setup with PNA and WR75 taper; measured results: (b) reflection Coefficients; (c) reflection Phases.

cell with soldered PIN diodes. The measurement setup using PNA and taper WR75 is shown in Figure 8(a). To control a full RRA, a controlling board is generally designed to control diode states. In this paper, only.

two unit cells with 8 diodes are measured, and the author only adopted a DC supplier to switch two DC levels (5 V and – 5V). The measured results are demonstrated in Figure 8(b). For "OFF" state, the measured reflection coefficients lose around 0.5 dB at frequencies lower of 14 GHz and nearly 1 dB at frequencies greater than 14 GHz compared to the simulated results. This discrepancy is resulted from the gaps between the unit cell and the waveguide which cause an echo or unwanted resonance and loss. The defective or inhomogeneous vias also contribute to this problem. However, the reflective phase for "OFF" state is still relatively agreeable with the simulation results. For "ON" state, when two patches are connected together, this effect is more severe, especially at frequencies greater than 13.6 GHz. As shown in Figure 8(b), the measured reflection coefficient has a loss more from 13 GHz and drop significantly from 14 GHz, which leads to a large discrepancy between simulated and measured phases from 13.6 GHz. To avoid the gap between metal walls and the unit cell and remove most of the unwanted effects at high frequencies, a square ring of small vias can be adopted to create a virtual wall around the unit cell. However, as aforementioned, lack of specific equipment and chemicals makes it impossible. A comparison of the proposed unit cell with some related reports is presented in Table 2. From this table, it can be seen that the proposed unit cell shows an excellent performance in terms of bandwidth

Table 2: Comparison of unit cells with 1-bit control using PIN diodes.

Ref./Year	f (GHz)/BW	No of PIN diodes	No of substrates/thickness (mm)	$\|\Gamma\|$ ON/OFF (dB)	Polarization
[26]/2016	13.5–15; 10.5%	2	2, NP	−0.5 to −1; −0.3 to −0.7	DL, CP
[28]/2016	12−−14.5; 18.8%	4	4, NP	−0.5 to −1; −0.5 to 1	DL, CP, RP
[31]/2019	4.7−−5.3; 12%	1	2, 2.7	−0.1 to −0.9; −0.1 to −0.9	SL
[35]/2021	11.6–14.3; 20.8%	2	3, 3.357	1.1.6	SL
This work	**10.4-15.7; 40.6%**	**4**	**2, 3.405**	**−0.9 to −1.4; 0.05**	**DL, CP**

The criterion for BW is the phase difference of $180^{o} \pm 20^{o}$. NP : not published, SL : single linear polarization, DL : dual linear polarization, CP : circular polarization, and PR : polarization rotation. Values in bold highlight our proposed work.

compared to the other works. This reflects that the structure of the unit cell avoids the mismatching between two components connected by diode and eliminate the effect of the DC-bias structure. For reflection coefficient, due to using 4 diodes, the insert loss is high for state "ON," just lower the work in [20]. However, for "OFF" state, they show the best performance. The unit cell also has an excellent average reflection coefficient, less than 0.7 dB. These results come from the proper DC-bias structure, material RT5880 with a low loss tangent, and low insert loss PIN diodes.

4. Conclusion

A fully multipolarized configurable unit cell with 1-bit control for RRAs is proposed. By using four PIN diodes with two states ON and OFF, the phase of the element is manipulated in a 180^{o} range. The impacts of DC-bias structures on the unit cell performance are carefully investigated and maximally eliminated. The simulated results demonstrate that the unit cell achieves a bandwidth of more than 40% at band *X* and Ku for both dual linear and circular polarizations while having high isolation between cross and copolarizations. The unit cell is also fabricated and experimentally characterized by using WR75 tapers calibrated by the TRL method. The measurement is also in agreement with those simulated for frequency band lower 13.6 GHz. The obtained performances of the designed unit cell have demonstrated the great potential to enhance the bandwidth of the 1-bit RRAs.

Data Availability

The data used to support the findings of this study are included within the article.

Conflicts of Interest

The authors declare that there are no conflicts of interest regarding the publication of this paper.

References

[1] Z. Liu, X. Lei, J.-M. Wu, and Z.-J. Xu, "Dual-mode circular polarization selective surface cell for single-layer dual-band circularly polarized reflectarray," *International Journal of Antennas and Propagation*, vol. 2019, Article ID 7143274, 7 pages, 2019.

[2] J. Ren and W. Menzel, "Millimeter-wave single-layer dual-frequency reflectarray antenna," *International Journal of Antennas and Propagation*, vol. 2017, Article ID 6170863, 4 pages, 2017.

[3] S. H. Zainud-Deen, N. A. El-Shalaby, S. M. Gaber, and H. A. Malhat, "Circularly polarized transparent microstrip patch reflectarray integrated with solar cell for satellite applications," *International Journal of Microwave Science and Technology*, vol. 2016, Article ID 6102530, 7 pages, 2016.

[4] S. Costanzo, F. Venneri, A. Borgia, and G. D. Massa, "A single-layer dual-band reflectarray cell for 5G communication systems," *International Journal of Antennas and Propagation*, vol. 2019, Article ID 9479010, 9 pages, 2019.

[5] H. D. Cuong, M.-T. Le, and N. Q. Dinh, "A reflectarray antenna using crosses and square rings for 5G millimeter-wave application," in *Proceedings of the 2020 International Conference on Advanced Technologies for Communications (ATC)*, pp. 126–130, IEEE, Nha Trang, Vietnam, October 2020.

[6] J. Huang, "Bandwidth study of microstrip reflectarray and a novel phased reflectarray concept," in *Proceedings of the IEEE Antennas and Propagation Society International Symposium*, vol. 1, pp. 582–585, IEEE, Newport Beach, CA, USA, June1995.

[7] Y. Liu, Y. J. Cheng, X. Y. Lei, and P. F. Kou, "Millimeter-wave single-layer wideband high-gain reflectarray antenna with ability of spatial dispersion compensation," *IEEE Transactions on Antennas and Propagation*, vol. 66, no. 12, pp. 6862–6868, 2018.

[8] J. H. Yoon, Y. J. Yoon, W. S. Lee, and J. H. So, "Broadband microstrip reflectarray with five parallel dipole elements," *IEEE Antennas and Wireless Propagation Letters*, vol. 14, pp. 1109–1112, 2015.

[9] E.-C. Choi and S. Nam, "W-band low phase sensitivity reflectarray antennas with wideband characteristics considering the effect of angle of incidence," *IEEE Access*, vol. 8, Article ID 111073, 2020.

[10] X. Wang, X. Huang, X. Jin, and C. Cheng, "Gain enhancement for low cost planar reflectarray antenna using hybrid elements," *International Journal of RF and Microwave Computer-Aided Engineering*, vol. 30, no. 8, Article ID e22204, 2020.

[11] S. Costanzo, F. Venneri, and G. D. Massa, "Modified minkowski fractal unit cell for reflectarrays with low sensitivity to mutual coupling effects," *International Journal of Antennas and Propagation*, vol. 2019, Article ID 4890710, 11 pages, 2019.

[12] S. Buzzi, E. Grossi, M. Lops, and L. Venturino, "Foundations of MIMO Radar Detection Aided by Reconfigurable Intelligent Surfaces," 2021, http://arXiv.org/abs:2105.09250.

[13] Z. Zhang, L. Dai, and C. Liu, "Active RIS vs. passive RIS: which will prevail in 6G?," 2021, http://arXiv.org/abs:2103.15154.

[14] C. You and R. Zhang, "Wireless communication aided by intelligent reflecting surface: active or passive?" *IEEE Wireless Communications Letters*, vol. 10, no. 12, pp. 2659–2663, 2021.

[15] M. I. Abbasi, M. Y. Ismail, M. R. Kamarudin, and Q. H. Abbasi, "Reconfigurable reflectarray antenna: a comparison between design using PIN diodes and liquid crystals," *Wireless Communications and Mobile Computing*, vol. 2021, Article ID 2835638, 8 pages, 2021.

[16] F. Venneri, S. Costanzo, and G. D. Massa, "Design and validation of a reconfigurable single varactor-tuned reflectarray," *IEEE Transactions on Antennas and Propagation*, vol. 61, no. 2, pp. 635–645, 2012.

[17] M. E. Trampler, R. E. Lovato, and X. Gong, "Dual-resonance continuously beam-scanning X-band reflectarray antenna," *IEEE Transactions on Antennas and Propagation*, vol. 68, no. 8, pp. 6080–6087, 2020.

[18] S. Montori, L. Marcaccioli, R. V. Gatti, and R. Sorrentino, "Constant-phase dual polarization MEMS-based elementary cell for electronic steerable reflectarrays," in *Proceedings of the European Microwave Conference (EuMC)*, pp. 033–036, IEEE, Rome, Italy, October 2009.

[19] O. Bayraktar, O. A. Civi, and T. Akin, "Beam switching reflectarray monolithically integrated with RF MEMS switches," *IEEE Transactions on Antennas and Propagation*, vol. 60, no. 2, pp. 854–862, 2011.

[20] K. Q. N. T. R. Henderson and N. Ghalichechian, "Steerable reflectarray using tunable height dielectric for high-power applications," in *Proceedings of the 2020 14th European Conference on Antennas and Propagation (EuCAP)*, pp. 1–4, IEEE, Copenhagen, Denmark, March 2020.

[21] D. M. Pozar, "Bandwidth of reflectarrays," *Electronics Letters*, vol. 39, no. 21, pp. 1490-1491, 2003.

[22] H. Yang, F. Yang, S. Xu, and M. Li, "A study of phase quantization effects for reconfigurable reflectarray antennas," *IEEE Antennas and Wireless Propagation Letters*, vol. 16, pp. 302–305, 2016.

[23] H. Kamoda, T. Iwasaki, J. Tsumochi, T. Kuki, and O. P. Hashimoto, "60-GHz electronically reconfigurable large reflectarray using single-bit phase shifters," *IEEE Transactions on Antennas and Propagation*, vol. 59, no. 7, pp. 2524–2531, 2011.

[24] A. Clemente, L. Dussopt, R. Sauleau, P. Potier, and P. Pouliguen, "1-Bit reconfigurable unit cell based on PIN diodes for transmit-array applications in X-Band," *IEEE Transactions on Antennas and Propagation*, vol. 60, no. 5, pp. 2260–2269, 2012.

[25] L. Di Palma, A. Clemente, L. Dussopt, R. Sauleau, P. Potier, and P. Pouliguen, "1-bit reconfigurable unit cell for Ka-band transmitarrays," *IEEE Antennas and Wireless Propagation Letters*, vol. 15, pp. 560–563, 2015.

[26] H. Yang, F. Yang, S. Xu, M. Li, X. Cao, and J. Gao, "A 1-bit multipolarization reflectarray element for reconfigurable large-aperture antennas," *IEEE Antennas and Wireless Propagation Letters*, vol. 16, pp. 581–584, 2016.

[27] H. Yang, F. Yang, S. Xu et al., "A 1-bit 10×10 reconfigurable reflectarray antenna: design, optimization, and experiment," *IEEE Transactions on Antennas and Propagation*, vol. 64, no. 6, pp. 2246–2254, 2016.

[28] M. T. Zhang and S. J. Gao, "Design of novel reconfigurable reflectarrays with single-bit phase resolution for Ku-band satellite antenna application," *IEEE Transactions on Antennas and Propagation*, vol. 64, no. 5, pp. 1634–1641, 2016.

[29] X. Pan, F. Yang, S. Xu, and M. Li, "Mode analysis of 1-bit reflectarray element using pin diode at w-band," in *Proceedings of the 2017 IEEE International Symposium on Antennas and Propagation & USNC/URSI National Radio Science Meeting*, pp. 2055-2056, IEEE, San Diego, CA, USA, July 2017.

[30] H. Yang, F. Yang, X. Cao et al., "A 1600-element dual-frequency electronically reconfigurable reflectarray at X/Ku-band," *IEEE Transactions on Antennas and Propagation*, vol. 65, no. 6, pp. 3024–3032, 2017.

[31] J. Han, L. Li, G. Liu, Z. Wu, Y. Shi, and W. P. Letters, "A wideband 1 bit 12×12 reconfigurable beam-scanning reflectarray: design, fabrication, and measurement," *IEEE Antennas and Wireless Propagation Letters*, vol. 18, no. 6, pp. 1268–1272, 2019.

[32] M. Wang, S. Xu, F. Yang, and M. Li, "A 1-bit bidirectional reconfigurable transmit-reflect-array using a single-layer slot element with PIN diodes," *IEEE Transactions on Antennas and Propagation*, vol. 67, no. 9, pp. 6205–6210, 2019.

[33] X. Pan, F. Yang, S. Xu, and M. Li, "A 10240-element reconfigurable reflectarray with fast steerable monopulse patterns," *IEEE Transactions on Antennas and Propagation*, vol. 69, no. 1, pp. 173–181, 2020.

[34] F. Wu, R. Lu, J. Wang, Z. H. Jiang, W. Hong, and K. M. Luk, "A circularly polarized 1-bit electronically reconfigurable reflectarray based on electromagnetic element rotation," *IEEE Transactions on Antennas and Propagation*, vol. 69, no. 9, pp. 5585–5595, 2021.

[35] B. Xi, Y. Xiao, K. Zhu, Y. Liu, H. Sun, and Z. Chen, "1-Bit Wideband Reconfigurable Reflectarray Design in Ku-Band," *IEEE Access*, vol. 10, 2021.

[36] X. Yang, S. Xu, F. Yang, and M. Li, "Design of a 2-bit reconfigurable reflectarray element using two MEMS switches," in *Proceedings of the 2015 IEEE International Symposium on Antennas and Propagation & USNC/URSI National Radio Science Meeting*, pp. 2167-2168, IEEE, Vancouver, BC, Canada, July 2015.

[37] B. D. Nguyen, V.-S. Tran, L. Mai, and P. Dinh-Hoang, "A two-bit reflectarray element using cut-ring patch coupled to delay lines," *REV Journal on Electronics and Communications*, vol. 6, no. 1-2, p. 4, 2016.

[38] L. Dai, B. Wang, M. Wang et al., "Reconfigurable intelligent surface-based wireless communications: antenna design, prototyping, and experimental results," *IEEE Access*, vol. 8, Article ID 45923, 2020.

[39] R. Pereira, R. Gillard, R. Sauleau, P. Potier, T. Dousset, and X. Delestre, "Dual linearly-polarized unit-cells with nearly 2-bit resolution for reflectarray applications in X-band," *IEEE Transactions on Antennas and Propagation*, vol. 60, no. 12, pp. 6042–6048, 2012.

[40] M. Cerveny, K. L. Ford, and A. Tennant, "Reflective switchable polarization rotator based on metasurface with PIN diodes," *IEEE Transactions on Antennas and Propagation*, vol. 69, no. 3, pp. 1483–1492, 2020.

[41] R. S. Malfajani and B. A. Arand, "Dual-band orthogonally polarized single-layer reflectarray antenna," *IEEE Transactions on Antennas and Propagation*, vol. 65, no. 11, pp. 6145–6150, 2017.

[42] J. H. Yoon, Y. J. Yoon, W. S. Lee, and J. H. So, "Square ring element reflectarrays with improved radiation characteristics by reducing reflection phase sensitivity," *IEEE Transactions on Antennas and Propagation*, vol. 63, no. 2, pp. 814–818, 2014.